

# MULTIHARMONIC BUNCHER FOR THE ISOLDE SUPERCONDUCTING RECOIL SEPARATOR PROJECT\*

J. L. Muñoz<sup>†</sup>, I. Bustinduy, S. Varnasseri, P. González, A. Kaftoosian, L. Catalina-Medina  
Consorcio ESS-Bilbao, Zamudio, Bizkaia, Spain  
I. Martel, University of Huelva, Huelva, Spain

## Abstract

The ISOLDE Superconducting Recoil Separator (ISRS) is based on a very compact particle storage ring of only 3.5 m in diameter. This instrument will be coupled with present and future detector systems of the HIE-ISOLDE facility. The injection of the HIE-ISOLDE beam into this ring requires a more compact bunch structure, so a Multi-Harmonic Buncher (MHB) device is proposed for this task. The MHB will operate at a frequency of 10.128 MHz, which is a 10% of the linac frequency, and would be installed before the RFQ. The MHB is designed as a two electrodes system, and the MHB signal, composed for the first four harmonics of the fundamental frequency, is fed into the electrodes that are connected to the central conductor of a coaxial waveguides. The full design of the MHB is presented, including electromagnetic optimization of the electrode shape, optimization of the weights of each of the harmonic contribution, mechanical and thermal design of the structure. The RF generation and electronics to power up the device are also presented. A solution that generates directly the composed signal and is then amplified by a solid state power amplifier is also presented in this contribution.

## INTRODUCTION

The HIE-ISOLDE [1] facility at CERN can accelerate more than 1000 isotopes of about 70 elements at collision energies up to 10 MeV/A, thus making it an ideal testbench to probe nuclear theories by selecting optimum (N, Z) combinations.

The “ISOLDE Superconducting Recoil Separator” (ISRS) [2, 3] is a novel high-resolution spectrometer based on multi-function superconducting canted cosine theta magnets. This device will extend the physics program to more exotic isotopes produced in the secondary target. It will use focal plane spectroscopy with particle and photon detection using different detector devices at HIE-ISOLDE. The ISRS device consists on a ring composed of an array of iron-free superconducting multifunction magnets (SCMF) cooled by cryocoolers [4].

The HIE-ISOLDE linac operates at an RF frequency of 101.28 MHz, which results in a bunch separation of 9.87 ns. For operation of the ISRS, a longer separation is required. This can be achieved by inserting a pre-buncher before the RFQ. If the buncher operates at a frequency of 1/10th ( $f=10.128$  MHz), then the bunch separation will be increased

by a factor of ten, but at the same time the beam will be bunched at an exact fraction of the linac RF frequency, so it can be transmitted and accelerated by the RFQ and the rest of the linac.

Within the framework of the ISRS collaboration, a MHB prototype will be designed and built. The device will comply with ISOLDE specifications. At this stage of the project, the cavity will be tested in ESS-Bilbao injector, so diagnostics and other elements are also being developed [5].

## MULTIHARMONIC BUNCHER DESIGN

The common technology for a buncher for radioactive beams in that frequency range is a Multi-Harmonic Buncher (MHB) [6–9]. To bunch a continuous beam to a certain RF frequency  $f$ , the optimum field time profile is a saw-tooth wave profile of frequency  $f$  [6], with a linear ramp of field centered at the middle of the bunch. The saw-tooth profile can be synthesized by summing up the first harmonics of its Fourier expansion. Usually, four harmonic terms are enough to generate an adequate approximation of the wave shape. In the MHB, this electric field is applied to two electrodes powered up with the combined multiharmonic RF wave. The field in the gap between the electrodes will be as uniform as possible, and it will be modulated by the MHB wave. In a real device the electric field between the electrodes depends on the electrode geometry and the aperture needed for the beam, so the actual performance of the MHB will be lower than the ideal one.

The buncher electrode geometry is usually designed by assuming a constant voltage [6–9]. In this way the field spatial distribution can be computed as an electrostatics problem. The field is taken as an amplitude that is then modulated by the four harmonic components, each one with the adequate weight, to obtain the composed saw-tooth profile in the time domain. Beam dynamics simulations are then run to evaluate the bunching efficiency. For low frequencies the differences in the electric field shape between an electrostatics and a RF calculations are very low. The design procedure and the computational tools used have already been reported in [10].

## Electrode Geometry

In Fig. 1 the electric field maps of two models are shown. The original model (named here Fraser model) is the one described in [7], while the wedge shaped model is a modification of this one. The gap in both cases is of 5 mm and the aperture is of 20 mm. The electric field profile along

\* This research is funded by the Next Generation EU–Recovery and Resilience Facility (RRF).

<sup>†</sup> jlmunoz@essbilbao.org

the axis for both models is shown in Fig. 2 for an voltage difference of 1 kV between electrodes.

### Beam Dynamics and Bunching Efficiency

The axisymmetric field maps obtained for the models defined in the previous section are exported and combined to produce the multiharmonic electric field. The field map exported corresponds to the electrostatic field distribution, but due to the low frequencies considered the field distribution is assumed to be the same for the fundamental RF frequency of  $f=10.128$  MHz as well as for the next 3 harmonics  $2f$ ,  $3f$  and  $4f$ . From the electric field map,  $E_0$ , obtained with a voltage difference of 1 kV, the composed MHB field is then obtained as:

$$E_{MHB}(r, z) = \left(\frac{V_0}{1000}\right)E_0(r, z) \sum_{n=1}^4 (a_n \sin n\omega t) \quad (1)$$

The harmonic weights  $a_n$  that appear in Eq. (1) will in practice be optimization parameters, but for the present paper the values chosen are the first Fourier expansions terms of the linear saw-tooth profile:  $a_0 = 1$ ,  $a_1 = -0.428$ ,  $a_2 = 0.215$  and  $a_4 = -0.101$ . For particle tracking simulations (using GPT code [11]) take as input the ISOLDE beam parameters described for example in [7]:  $A/q=4.5$ ,  $\beta=0.00328$ ,  $\epsilon_x, \epsilon_y=0.62$  mm mrad and a beam intensity of 1 nA.

The beam is propagated through the MHB and down the line in a multiparticle simulation. At a certain longitudinal distance  $z$  from the cavity center (measured from the middle of the gap between electrodes, a certain bunching efficiency figure of merit can be calculated. This is an statistical magnitude that is useful to compare among different cavity designs or operational parameters. This is done in the following way: first, the  $z$  coordinates of all particles are discretized in buckets  $Z$  (for example of  $\Delta z=10$  mm). Then, the distribution of times for all the particles arriving at  $Z$  are collected. From the mode of the distribution a window of  $\tau = 1/f$  is then selected. The bunching efficiency at  $z$  is the ratio of the number of particles arriving at the most frequent value divided by the total.

For the models described above, the bunching efficiency as a function of the distance from the center is shown in Fig. 3. Two different effective voltage,  $V_0$  in Eq. (1), are considered, 520 V and 1500 V. Results are very similar for both geometries. As expected, the maximum longitudinal focusing length decreases as voltage is increased. This is shown more clearly in Fig. 4, where this dependence is shown as color maps of the bunching efficiency.

So, depending on where in the REX-ISOLDE line the MHB could be installed, a different value for the optimum focusing length would be needed. This length could be tuned up changing the voltage between electrodes, that in the end is a result of the RF power fed into the electrodes, as described in the following section.

### MHB 3D DESIGN

In the real cavity, the voltage between the electrodes and the spatial distribution of the electric field used in the previous section calculations are the result of applying the com-

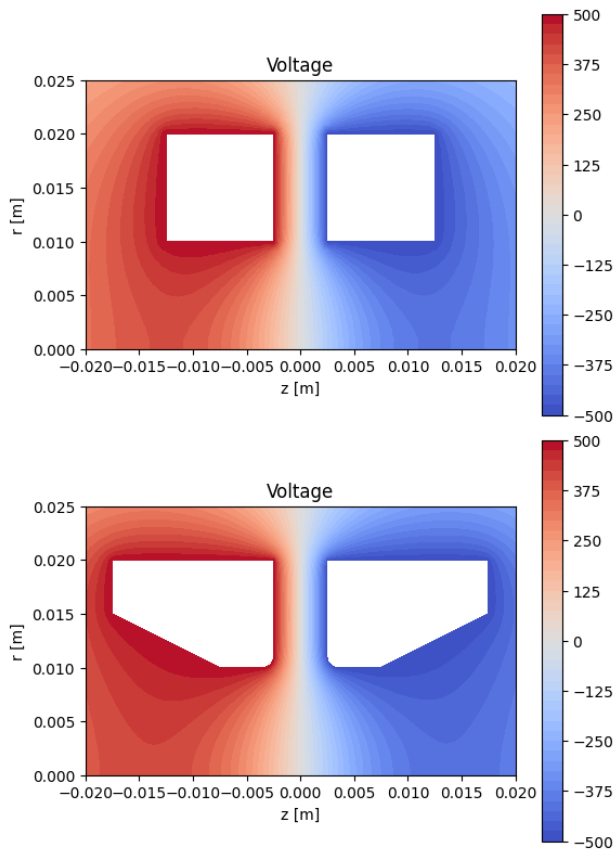


Figure 1: Electric field maps for the axisymmetric models for the initial Fraser geometry (top) and for a wedge shape model (bottom). Voltage between electrodes is 1 kV in both cases.

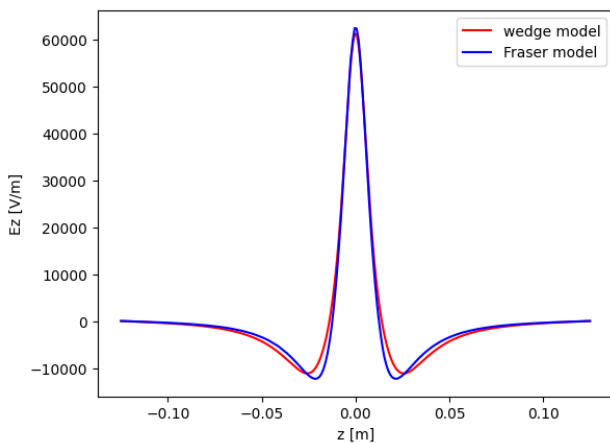


Figure 2: Electric field profile along the beam axis for the Fraser and wedge electrode models. Voltage between electrodes is 1 kV in both cases.

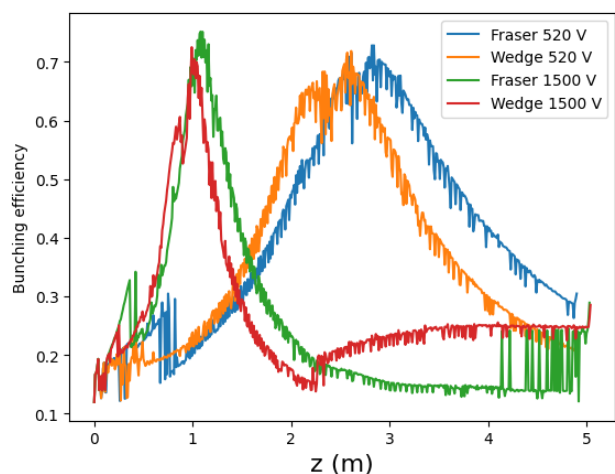


Figure 3: Bunching efficiency (see text for details) computed for the Fraser and wedge models as a function of the distance from the buncher center, for effective voltages of 520 V and 1500 V.

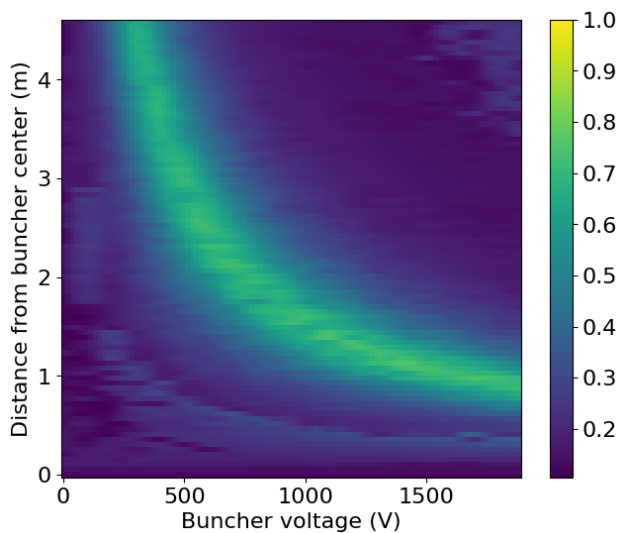


Figure 4: Color map representing bunching efficiency for the wedge model as a function of distance from buncher center and effective voltage between electrodes.

binned multiharmonic RF wave, of a certain power, to the electrodes. The electrodes body are connected to the internal conductor of a coaxial line, while the external coaxial are grounded to the cavity body. The signals fed into each of the electrodes have a phase difference of  $\pi$  radians. The coaxial internal conductor (electrodes stem) has a radius of  $a = 4$  mm, and the external conductor has an inner radius of  $b = 2.3023a = 9.209$  mm corresponding to a line impedance of  $50 \Omega$ .

In Fig. 5 the 3D electromagnetic model is shown, together with the simulated field map for the fundamental frequency. The field profiles along the axis are shown in Fig. 6 to verify that the profiles for the four harmonics, and for the electrostatics case, are almost identical. The RF power equivalent to

a voltage difference of 1 kV between electrodes is of 625 W through each coaxial line, to a total of 1250 W for the fundamental harmonic. For harmonics  $n=2,3$  and 4 additional signals of the corresponding weights should be fed into the system, for a total power of 2.2 kW for an equivalent voltage of 1 kV.

The RF power would heat up the copper electrodes and coaxial line. According to simulations, for the total power level of 2.2 kW, the temperature of the electrodes and cavity barely increases above room temperature, so active cooling is planned for the MHB.

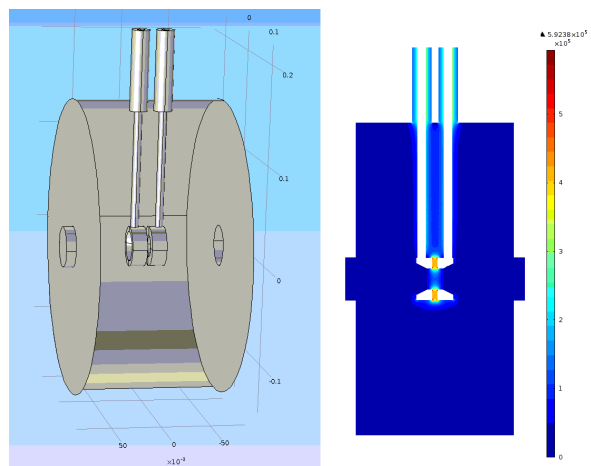


Figure 5: 3D electromagnetic model of the MHB with wedge electrodes. The field map corresponds to a frequency domain calculation at the base frequency of 10.128 MHz.

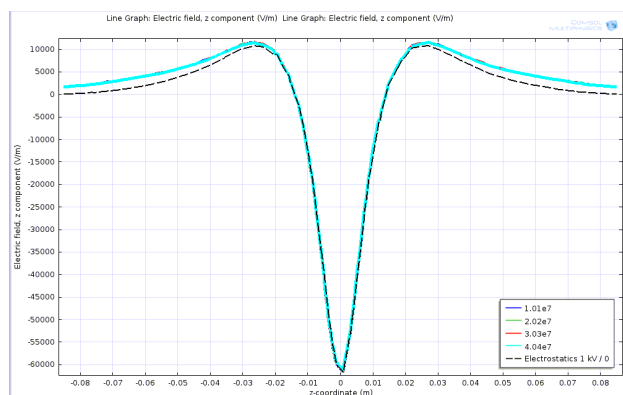


Figure 6: Field profiles, computed with the 3D electromagnetic model, for the four harmonics and for the electrostatic case. The differences are very small.

## RF SIGNAL GENERATION

The common technique for generating the sawtooth waveform needed for bunching is to use the harmonics of its Fourier expansion and combining them with proper amplitude and phase. The reason to generate sawtooth waveform by summing its Fourier components is that it will be more flexible to choose the high-power amplification system to

amplify either by a wide-band amplifier or four narrowband amplifiers dedicated to each harmonic. More importantly, in case of using a sawtooth signal directly, an ideal amplifier with constant gain and very high linearity and wide bandwidth would be needed to amplify the signal and also maintain the sawtooth profile, this is not feasible with the existing high-power amplifiers. Even if such amplifier was available, still the signal is prone to distortion by passing through BALUN and the cavity itself. In the other hand, by using the harmonics as the basic elements of the sawtooth waveform, any amplitude and phase variations happening on the signal along the path from source up to the cavity can be measured at the cavity pickup and be compensated through a feedback or feed-forward system. Throughout this process, an adequate sawtooth signal will be regenerated inside the MHB cavity with sufficient power level. The Fourier components used for the signal generation are the ones described for Eq. (1).

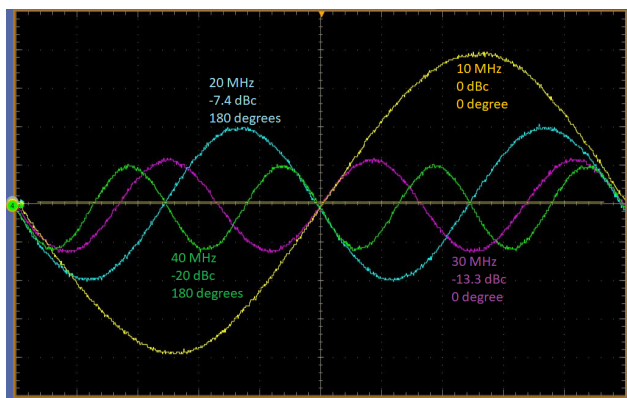


Figure 7: The measurement of the four harmonics used to generate the sawtooth signal.

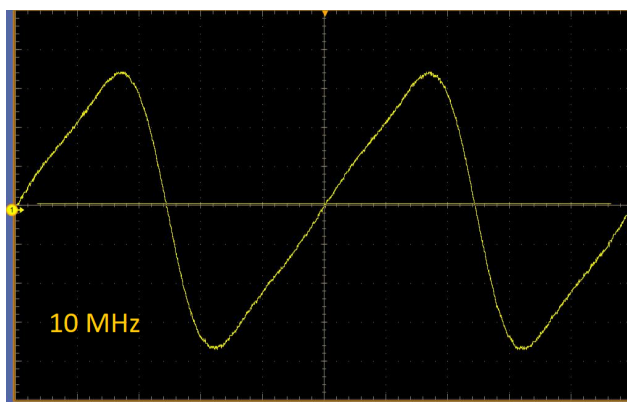


Figure 8: The measurement of the sawtooth signal generated by combining the four harmonics.

Figures 7 and 8 show the harmonics used in the test bench and the sawtooth signal generated by adding those harmonics by means of a power combiner.

A simplified block diagram of the test bench at ESS-Bilbao is shown in Fig. 9. Four signal generators are used to

generate the harmonics. Attenuators are placed at the power combiner inputs to increase the isolation between the signals. The lower the power, the more isolation is needed. Phase and amplitude of the 10MHz signal are considered as reference and the other 3 signals are adjusted accordingly. The signal generated will be distorted at the output of the amplifiers depending on linearity of the amplifiers. A voltage-controlled attenuator is used as an output power tuner, also power levels of each harmonic can be monitored by a spectrum analyser so the relative power levels can be adjusted.

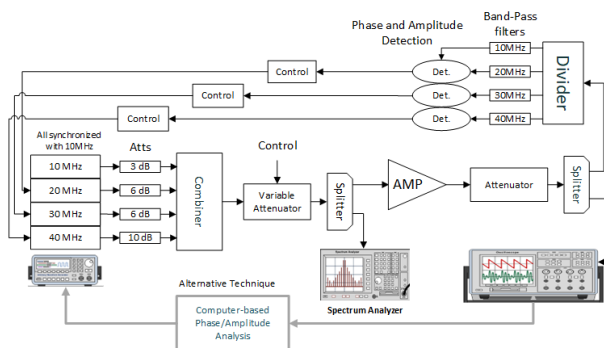


Figure 9: Simplified block diagram of the test bench.

## ESS-BILBAO TEST BENCH

After fabrication, it is foreseen to test the MHB with the ESS-Bilbao injector. For that, an Ion Test Bench (ITB) consisting of some diagnostics components such as an ACCT for current measurements and a Fast Faraday Cup for the bunch length measurements is under design. The Fast Faraday Cup is of the stripline type, with wide band frequency response for precise measurement of bunch length [5]. The ITB diagnostics components can also help the characterization of the MHB bunching and beam loss before its final installation in ISOLDE-ISRS [3].

## CONCLUSION

A preliminary design for a MHB is presented. Within the ISRS project, a prototype of this cavity will be fine-designed and built. The device, together with the corresponding RF power signal generation and diagnostics, will be tested at ESS-Bilbao injector.

## REFERENCES

- [1] M.J.G. Borge, “Highlights of the ISOLDE facility and the HIE-ISOLDE project”, *Nucl. Instrum. Methods Phys. Res., Sect. B*, vol. 376, pp. 408–412, 2016. doi:10.1016/j.nimb.2015.12.048
- [2] I. Martel, O. Tengblad, J. Cederkall, “Design study of a Superconducting Recoil Separator for HIE-ISOLDE”, CERN, Geneva, Switzerland, Rep. CERN INTC-I-228, 2021. <https://cds.cern.ch/record/2749891/files/INTC-I-228.pdf>
- [3] I. Martel *et al.*, “An innovative Superconducting Recoil Separator for HIE-ISOLDE”, *Nucl. Instrum. Methods Phys. Res.*,



- Sect. B*, vol. 541, pp. 176-179, 2023.  
doi:10.1016/j.nimb.2023.05.052
- [4] C. Bontoiu, I. Martel, J. Resta-López, V. Rodin, C. P. Welsch, “Conceptual design of a novel and compact superconducting recoil separator for radioactive isotopes”, *Nucl. Instrum. Methods Phys. Res., Sect. A*, vol. 969, p. 164048, 2020.  
doi:10.1016/j.nima.2020.164048
- [5] S. Varnasseri *et al.*, “Stripline design of a fast Farady cup for the bunch length measurement at ISOLDE-ISRS”, presented at HB’23, Geneva, Switzerland, Oct. 2023. paper THAFP10, these proceedings.
- [6] J. Staples, “Reducing RFQ Output Emittance by External Bunching,” in *Proc. of Workshop on Post-Accelerator Issues at the IsoSpin Laboratory*, Berkeley, CA, USA, 27 - 29 Oct. 1993, see *Part. Accel.*, vol. 47, pp. 191-199, 1994.
- [7] M. A. Fraser, R. Calaga, and I.-B. Magdau, “Design Study for 10 MHz Beam Frequency of Post-accelerated RIBs at HIE-ISOLDE”, in *Proc. IPAC’13*, Shanghai, China, May 2013, paper THPWO076, pp. 3933–3935.
- [8] J. Labrador *et al.*, “Design of a Multi-harmonic Buncher for LINCE”, in *Proc. IPAC’14*, Dresden, Germany, Jun. 2014, pp. 508–510.  
doi:10.18429/JACoW-IPAC2014-MOPME059
- [9] D. M. Alt *et al.*, “Preparatory Investigations for a Low Frequency Prebuncher at ReA”, in *Proc. IPAC’14*, Dresden, Germany, Jun. 2014, pp. 3342–3345.  
doi:10.18429/JACoW-IPAC2014-THPME051
- [10] J. L. Muñoz, I. Bustinduy, P. J. González, and L. C. Medina, “Multi-Harmonic Buncher (MHB) Studies for Protons and Ions in ESS-Bilbao”, in *Proc. LINAC’22*, Liverpool, UK, Aug.-Sep. 2022, pp. 334-336.  
doi:10.18429/JACoW-LINAC2022-TUPOJ002
- [11] Pulsar Physics, General Particle Tracer,  
[www.pulsar.nl/gpt](http://www.pulsar.nl/gpt)